Available online at http://scik.org

J. Math. Comput. Sci. 11 (2021), No. 4, 4183-4202

https://doi.org/10.28919/jmcs/5806

ISSN: 1927-5307

OSCILLATORY FLOW OF A VISCOUS CONDUCTING FLUID THROUGH A UNIFORMLY MOVING VERTICAL CIRCULAR CYLINDER UNDER PRESSURE GRADIENT

K. CHAMUAH*, N. AHMED, K. CHOUDHURY

Department of Mathematics, Gauhati University, Guwahati-781014, India

Abstract: A study of a transient MHD mass transfer flow of a viscous incompressible and electrically conducting Newtonian non-Gray optically thin fluid through a vertical circular cylinder influenced by a time dependent periodic pressure gradient subject to a magnetic field applied in azimuthal direction, in the presence of a frequency parameter and periodic wall temperature is provided. The flow, heat and mass transfer governing equations are converted into ordinary differential equations by imposing some suitable transformations and solved in closed form using Bessel functions of order zero. Graphs depict the effects of various physical parameters on concentration, velocity, temperature field and on the coefficient of the skin friction, mass flux across a normal suction of the cylinder and the rates of heat and mass transfer at surface of the cylinder in the issue.

Keywords: MHD; mass flux; periodic wall temperature; mass diffusivity.

2010 AMS Subject Classification: 76W05.

*Corresponding author

E-mail address: kalyanchamuah60@gmail.com

Received April 2, 2021

1. INTRODUCTION

MHD viscous fluid flow through pipes is important in many fields of Science and Technology, including Bio-mechanics, Petroleum Industry, Drainage and Irrigation Engineering and so on. Many authors have investigated the problems of steady and unsteady flows of viscous incompressible fluids through cylinders with various cross sections under various flow geometries and physical aspects. Some of them are Kumari and Bansal [1], Drake [2], Varma et al. [3], Antimirov and Kolyshkin [4], Hughes and Young [5], Sankar et al. [6], Jain and Mehta [7] and Globe [8.] Several scholars, on the other hand, have looked into MHD flows and heat transfer in channels and circular pipes. Chamkha [9] looked at how two different applied pressure gradients (ramp and oscillating) affected unsteady laminar MHD flow and heat transfer in channels and circular pipes. Singh [10] gave an exact solution to the problem of MHD mixed convection periodic flow in a rotating vertical channel in the presence of heat radiation. Problems with MHD heat transfer and periodic wall temperature are also common. Israel-Cookey et al. [11] looked into MHD free convection and oscillating flow of an optically thin fluid surrounded by two horizontal porous parallel walls in the presence of periodic wall temperature. In addition, Reddy et al. [12] added periodic wall temperature to their problem.

In the context of geothermal power generation and drilling operations, studies of free convection flow along a vertical or horizontal cylinder are important because the free stream and buoyancy induced fluid velocities are of approximately the same order of magnitude. In the presence of a first-order chemical reaction, Machireddy [13] found a numerical solution to investigate the effects of radiation on MHD heat and mass transfer flow past a moving vertical cylinder. Ganesan and Loganathan [14] looked at the effects of radiation and mass transfer on the movement of an incompressible viscous fluid through a moving vertical cylinder. The study of flow and heat transfer in the vertical circular cylinder is a focus of investigation due to its wide range of practical applications such as solar collectors, electrical machineries, cooling system for electronic devices and other rotating system.

The effects of thermal radiation on heat and mass transfer are more significant in many system,

and they play a key role in the filtrations processes, design of spacecraft, nuclear reactors and the drying of porous material in textiles industries solar energy collector. Raju et al. [15] recently investigated the effect of thermal radiation on an unsteady free convection flow of water near four degree Celsius through a vertically moving porous plate by taking into account the effect of suction/injection. Gundagani et al. [16] investigated the effects of radiation on an unsteady MHD two-dimensional laminar mixed convective boundary layer flow along a vertically moving semi-infinite permeable plate with suction, embedded in a uniform porous medium, thus accounting for viscous dissipation. Rao et al.[17] looked at how radiation influenced the unsteady mass transfer flow of a chemically reacting fluid through a semi-infinite vertical plate in the presence of viscous dissipation. Recently, Ahmed and Dutta [18] carried out an analytical study of a laminar unsteady MHD flow past a vertical annulus in presence of thermal radiation under the influence of periodic wall temperature and pressure gradient. N. Ahmed [19] made a theoretical analysis of a steady MHD free convective flow on a vertical circular cylinder with Soret and Dufour effects.

The present investigation is concerned with the study of unsteady, MHD flow of Newtonian non-Gray optically thin fluid through a vertical circular cylinder in the presence of frequency parameter, time dependent pressure gradient and periodic temperature and concentration maintained at the wall of the cylinder. In the current work, such an attempt has been made.

2. BASIC EQUATIONS

The equations defining the motion of an incompressible, electrically conducting, viscous and radiating fluid in the presence of magnetic field are:

Equation of continuity:

$$\vec{\nabla}.\vec{q} = 0 \tag{1}$$

Momentum equation:

$$\rho\left[\frac{\partial\vec{q}}{\partial t'} + \left(\vec{q}.\vec{\nabla}\right)\vec{q}\right] = -\vec{\nabla}p' + \mu\nabla^2\vec{q} + \vec{J}\times\vec{B} + \rho\vec{g} \tag{2}$$

Energy equation:

$$\rho C_p \left[\frac{\partial T}{\partial t'} + \left(\vec{q}.\vec{\nabla} \right) T \right] = \kappa \nabla^2 T + \bar{\phi} - \vec{\nabla}.\vec{q}_r \tag{3}$$

Ohm's law for an electrically conducting fluid:

$$\vec{J} = \sigma \left(\vec{q} \times \vec{B} \right) \tag{4}$$

Species continuity equation:

$$\frac{\partial C}{\partial t'} + \left(\vec{q}.\vec{\nabla} \right) C = D_M \nabla^2 C \tag{5}$$

The nomenclature specifies all physical quantities.

3. MATHEMATICAL ANALYSIS

Consider a vertical circular cylinder of radius a with an unsteady laminar radiative flow of a viscous incompressible electrically conducting fluid. In Figure 1, z'-axis is used as the axis of the cylinder in a cylindrical polar coordinate $\left(r', \psi, z' \right)$. The fluid is influenced by a time dependent periodic pressure gradient as well as a magnetic field $\vec{B} = \left(0, B_o, 0 \right)$ applied in the azimuthal direction.

Our investigation is limited to the following assumptions in order to idealize the mathematical model of the problem:

i. Except for the density in the buoyancy force term, all fluid properties are constant.

ii. Energy dissipation due to viscous and ohmic dissipation is insignificant.

iii. The radiative heat flux in the vertical direction is insignificant in comparison to that in normal direction.

iv. The induced magnetic field can be ignored because the magnetic Reynolds number is so small.

v. The flow is parallel to the cylinder's axis.

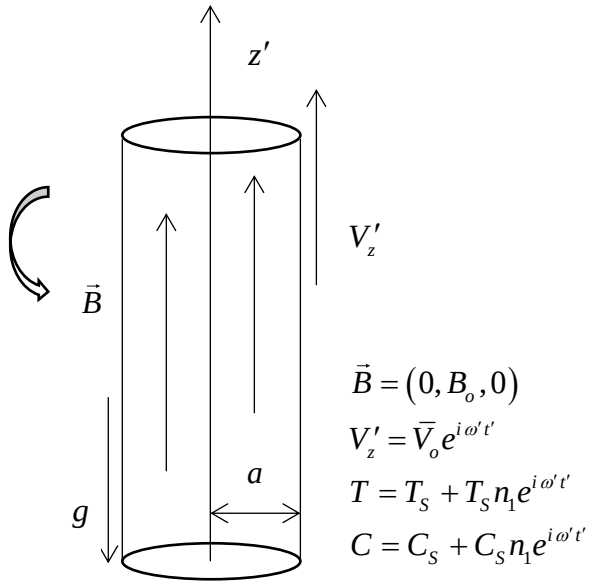

Figure1. Physical configuration

Let $\vec{q} = (0, 0, V_z')$ stand for fluid velocity, so that in (r', ψ, z') system the equation (1) becomes to

$$\frac{\partial V_z'}{\partial z'} = 0 \quad \text{which yields} \quad V_z' = V_z'(r', t') \tag{6}$$

From equations (2) and (6), we get

$$\rho \frac{\partial V_z'}{\partial t'} = -\frac{\partial p'}{\partial z'} + \mu\left(\frac{\partial^2 V_z'}{\partial r'^2} + \frac{1}{r'}\frac{\partial V_z'}{\partial r'}\right) - \sigma\mu_e^2 H_o^2 V_z' - \rho g \tag{7}$$

Where, $\vec{B} = \mu_e H_o \hat{\theta}$ and $\nabla^2 = \frac{\partial^2}{\partial r'^2} + \frac{1}{r'}\frac{\partial}{\partial r'}$

In the case of a static condition, equation (7) becomes

$$0 = -\frac{\partial p_s'}{\partial z'} - \rho_s g \tag{8}$$

The state equation as approximated by the classical Boussinesq approximation

$$\rho_s = \rho\left[1 + \beta(T - T_s) + \bar{\beta}(C - C_s)\right] \tag{9}$$

Momentum equation (7) on application of the equations (8) and (9), finally reduces to

$$\frac{\partial V_z'}{\partial t'} = -\frac{1}{\rho}\frac{\partial p'^*}{\partial z'} + \nu\left(\frac{\partial^2 V_z'}{\partial r'^2} + \frac{1}{r'}\frac{\partial V_z'}{\partial r'}\right) - \frac{\sigma\mu_e^2 H_o^2 V_z'}{\rho} + g\beta\left(T - T_s\right) + g\overline{\beta}\left(C - C_s\right) \tag{10}$$

Where $p'^* = p' - p_s'$

In view of the assumptions, the following reduced form of the equations (3) is obtained:

$$\rho C_p \frac{\partial T}{\partial t'} = \kappa\left(\frac{\partial^2 T}{\partial r'^2} + \frac{1}{r'}\frac{\partial T}{\partial r'}\right) - \frac{\partial q_r}{\partial r'} \tag{11}$$

Additionally, since the cylinder is infinite in both directions and so equation (5) becomes

$$\frac{\partial C}{\partial t'} = D_M\left(\frac{\partial^2 C}{\partial r'^2} + \frac{1}{r'}\frac{\partial C}{\partial r'}\right) \tag{12}$$

According to Cogley et al. [20] result, the rate of radiative heat flux in the optically thin limit for a non- Gray gas near equilibrium is given by the formula below:

$$\frac{\partial q_r}{\partial r} = 4I\left(T - T_s\right) \tag{13}$$

Where $I = \int_0^\infty \left(K_\lambda\right)_w \left(\frac{\partial e_{\lambda h}}{\partial T}\right)_w d\lambda$

Using equation (13) in the equation (11), we arrive at

$$\rho C_p \frac{\partial T}{\partial t'} = \kappa\left(\frac{\partial^2 T}{\partial r'^2} + \frac{1}{r'}\frac{\partial T}{\partial r'}\right) - 4I\left(T - T_s\right) \tag{14}$$

The pertinent boundary conditions are as follows:

$$\left.\begin{aligned} &V_z' = \overline{V}_o e^{iw't'},\ T = T_s + T_s n_1 e^{iw't'},\quad C = C_s + C_s n_1 e^{iw't'} \quad at\ r' = a \\ &V_z' = finite,\ T = finite,\ C = finite \quad at\ r' = 0 \end{aligned}\right\} \tag{15}$$

The following non-dimensional quantities are added to normalize the mathematical model:

$$\left.\begin{aligned} &V_z = \frac{V_z' a}{\nu},\ V_o = \frac{a\bar{V}_o}{\nu},\ \ r = \frac{r'}{a},\ z = \frac{z'}{a},\ \ p^* = \frac{p'^* a^2}{\mu\nu} \\ &t = \frac{t'\nu}{a^2},\ \ \omega = \frac{\omega' a^2}{\nu},\ \ \theta = \frac{T - T_s}{T_s},\ \ \phi = \frac{C - C_s}{C_s} \\ &Gr = \frac{g\beta a^3}{\nu^2} T_s,\ Gm = \frac{g\bar{\beta} a^3}{\nu^2} C_s,\ \ M = \mu_e H_o a\sqrt{\frac{\sigma}{\mu}} \\ &\Pr = \frac{\mu C_p}{\kappa},\ \ \ N = \frac{4Ia^2}{\mu C_p},\ \ \ Sc = \frac{\nu}{D_M} \end{aligned}\right\} \tag{16}$$

The non-dimensional forms of equations (10), (12) and (14) are as follows:

$$\frac{\partial V_z}{\partial t} = -\frac{\partial p^*}{\partial z} + \frac{\partial^2 V_z}{\partial r^2} + \frac{1}{r}\frac{\partial V_z}{\partial r} - M^2 V_z + Gr\theta + Gm\phi \tag{17}$$

$$\Pr\frac{\partial \theta}{\partial t} = \frac{\partial^2 \theta}{\partial r^2} + \frac{1}{r}\frac{\partial \theta}{\partial r} - N\Pr\theta \tag{18}$$

$$\frac{\partial \phi}{\partial t} = \frac{1}{Sc}\left(\frac{\partial^2 \phi}{\partial r^2} + \frac{1}{r}\frac{\partial \phi}{\partial r}\right) \tag{19}$$

With corresponding boundary conditions:

$$\left.\begin{aligned} &V_z = V_o e^{i\omega t},\ \theta = n_1 e^{i\omega t},\ \ \phi = n_1 e^{i\omega t}\ \ at\ r = 1 \\ &V_z = finite, \theta = finite,\ \phi = finite\ \ at\ r = 0 \end{aligned}\right\} \tag{20}$$

4. METHOD OF SOLUTION

Consider the concentration as $\phi(r,t) = f(r)e^{i\omega t}$ so that equation (19) becomes

$$r^2\frac{d^2 f}{dr^2} + r\frac{df}{dr} - r^2\gamma^2 = 0 \tag{21}$$

Where $\gamma^2 = i\omega Sc$

We substitute $z = ir\gamma,\ f(r) = f\left(\frac{z}{i\gamma}\right) = f_1(z)$ in equation (21) so that we obtain a Bessel equation of order 0:

$$z^2 \frac{d^2 f_1}{dz^2} + z \frac{df_1}{dz} + z^2 f_1 = 0 \tag{22}$$

Hence the solution of equation (22) is

$$f(r) = A_1 J_o(ir\gamma) \tag{23}$$

Where J_o is the Bessel function of first kind, of order 0.

As a result, for the concentration field, we get the following expression:

$$\phi(r,t) = A_1 I_o(r\gamma) e^{i\omega t} \tag{24}$$

Where I_o is zeroth order modified Bessel function of first kind.

$$A_1 = \frac{n_1}{I_o(\gamma)}$$

We define $\theta(r,t) = g(r) e^{i\omega t}$ and obtain the following expression for the temperature field

$$\theta(r,t) = A_2 I_o(r\eta) e^{i\omega t} \tag{25}$$

Where $\eta^2 = \Pr(i\omega + N)$ and $A_2 = \frac{n_1}{I_o(\eta)}$

Assume the pressure gradient to be periodic function of time. $-\frac{\partial p^*}{\partial z} = p_o e^{i\omega t}$ and defining V_z

as $V_z(r,t) = h(r) e^{i\omega t}$, the velocity of the fluid flow can be expressed as

$$V_z(r,t) = \left[A_3 I_o(r\delta) + \frac{p_o}{\delta^2} + A_4 I_o(r\eta) + A_5 I_o(r\gamma) \right] e^{i\omega t} \tag{26}$$

Where $\delta^2 = M^2 + i\omega$

$$A_3 = \frac{1}{I_o(\delta)} \left[V_o - \left\{ \frac{p_o}{\delta^2} + \left(\frac{Gr}{\delta^2 - \eta^2} + \frac{Gm}{\delta^2 - \gamma^2} \right) n_1 \right\} \right]$$

$$A_4 = \frac{GrA_2}{\delta^2 - \gamma^2}$$

$$A_5 = \frac{GmA_1}{\delta^2 - \gamma^2}.$$

5. MASS FLUX

The mass flux over every normal section of the cylinder can be calculated using the formula:

$$\overline{M} = \int_{r'=0}^{a}\int_{\psi=0}^{2\pi} \rho V_z' r' dr' d\psi = \rho a \nu \int_{r=0}^{1}\int_{\psi=0}^{2\pi} V_z r dr d\psi \tag{27}$$

The mass flux coefficient M_f is calculated using equation (27) as follows:

$$\begin{aligned} M &= \frac{\overline{M}}{\rho a \nu} = \int_{r=0}^{1}\int_{\psi=0}^{2\pi} V_z r dr d\psi \\ &= 2\pi e^{i\omega t}\left[\frac{1}{\delta}\left\{A_3 I_1(\delta) + \frac{p_o}{2\delta}\right\} + A_4 \frac{1}{\eta} I_1(\eta) + A_5 \frac{1}{\gamma} I_1(\gamma)\right] \end{aligned} \tag{28}$$

Where I_1 is modified Bessel functions of first kind, of order 1.

6. SKIN FRICTION

The Newton's law of viscosity, as shown below, gives the viscous drag per second area on the cylinder's surface:

$$\tau = -\mu \frac{\partial V_z'}{\partial r'}\Big]_{r'=a} = -\frac{\mu\nu}{a^2}\frac{\partial V_z}{\partial r}\Big]_{r=1} \tag{29}$$

The skin friction coefficient is calculated as follows:

$$\begin{aligned} C_f &= \frac{\tau}{\frac{\mu\nu}{a^2}} = -\frac{\partial V_z}{\partial r}\Big]_{r=1} \\ &= -e^{i\omega t}\left[A_3 \delta I_{-1}(\delta) + A_4 \eta I_{-1}(\eta) + A_5 \gamma I_{-1}(\gamma)\right] \end{aligned} \tag{30}$$

Where I_{-1} is modified Bessel functions of first kind, of order -1.

7. SHERWOOD NUMBER

Fick's law of mass diffusion determines the molecular mass flux M_W on the cylinder's surface is:

$$M_W = -D_M \left.\frac{\partial C}{\partial r'}\right]_{r'=a} = -D_M \left.\frac{C_S}{a}\frac{\partial \phi}{\partial r}\right]_{r=1} \tag{31}$$

According to equation (31), the coefficient of mass transfer on the surface of the cylinder in terms of Sherwood number is as follows:

$$\begin{aligned} Sh &= \frac{aM_W}{D_M C_S} = -\left[\frac{\partial \phi}{\partial r}\right]_{r=1} \\ &= -A_1 \gamma e^{i\omega t} I_{-1}(\gamma) \end{aligned} \tag{32}$$

8. NUSSELT NUMBER

The Fourier law of conduction gives the heat flux q^* from the cylinder's surface into the fluid area as follows:

$$q^* = -\kappa \left.\frac{\partial T}{\partial r'}\right]_{r'=a} = -\left.\frac{\kappa T_S}{a}\frac{\partial \theta}{\partial r}\right]_{r=1} \tag{33}$$

The heat transfer coefficient (Nusselt number) on the cylinder's surface is

$$\begin{aligned} Nu &= \frac{q^* a}{\kappa T_S} = -\left[\frac{\partial \theta}{\partial r}\right]_{r=1} \\ &= -A_2 \eta e^{i\omega t} I_{-1}(\eta) \end{aligned} \tag{34}$$

9. RESULTS AND DISCUSSIONS

Numerical calculations from the current investigation are valuable from a physical standpoint. Variations in the temperature field, velocity field, concentration field , mass flux, Sherwood number, Nusselt number, coefficient of skin friction, and different flow parameters such as frequency parameter ω , Prandtl number Pr, solutal Grashof number Gm, thermal Grashof

number Gr, Schmidt number Sc, magnetic parameter M are graphically depicted in Figures 2 to 15, while the values of other quantities are chosen at random.

In Figures 2 and 3, the temperature profiles are illustrated. These diagrams show how Pr and ω affect the temperature field. Figure 2 depicts the effect of changing the value of Pr on the temperature field. This figure shows that when the fluid's thermal diffusivity is decreased, the flow accelerates, which may be due to the fact that low thermal diffusivity causes a corresponding increase in the kinetic energy of the fluid's molecules. In addition, as shown in Figure 3, the frequency parameter has a tendency to lower fluid temperature. It is worth nothing that the fluid temperature drops as the temperature on the cylinder's surface oscillates. As a result, the frequency parameter serves as a useful regulatory mechanism for preserving the desired temperature field.

Figures 4 to 5 show the effects of M and Gm on fluid velocity. Figure 4 shows that increasing the value of the magnetic parameter M causes the fluid flow to slow down. The strength of the applied magnetic field is determined by the magnetic parameter. The interaction of the magnetic field and the fluid velocity causes the appearance of a resistive force known as Lorentz force when an azimuthal magnetic field is applied. The Lorentz force becomes dominant as the magnetic field strength increases, causing the fluid motion to slow down. Figure 5 shows that as the value of the solutal Grashof number Gm increases, the velocity profile rises as well. The ratio of a species' buoyancy force to its viscous hydrodynamic force is defined by the solutal Grashof number. As a result of the large rise in species buoyancy force, an increase in Gm shows small viscous effects in the momentum equation, and the fluid moves freely. Thus, our observation from Figure 5 is confirmed by physical reality.

The concentration profiles for ω and Sc variance are shown in Figures 6 and 7. Figure 6 shows that as the frequency parameter's magnitude increases, so does the fluid concentration. Figure 7 depicts the increase in concentration field caused by an increase in Sc. It is worth noting that as Sc rises, mass diffusivity decreases. As a result, high mass diffusivity causes fluid concentration to slow down.

Figure 8 and 9 show the variation in mass flux with time under the influence of Gm and Pr. These figures exhibit a common feature that the behaviour of mass flux under the effects of these parameters is periodic due to the pressure gradient being periodic function of time. Furthermore, we can see from these graphs that the magnitude of mass flux, which measures the rate at which mass is transmitted, increases as Gm and Pr increase caused by an increase in solutal buoyancy force and thermal diffusivity.

Figures 10 and 11 show how changes in Gm and Gr affect skin friction on the cylinder's surface as times goes on. Figures 10 and 11 shows that the direction of skin friction changes on a regular basis. This could be explained by the fact that the pressure gradient is periodic. Figure 11 show that as Gr rises, skin friction rises in the direction of fluid flow, which may be due to the buoyancy force acting on the fluid. However, due to the increase in solutal buoyancy force, the magnitude of skin friction increases as Gm increases (see Figure 10).

Figures 12 and 13 show how Pr and ω affect the rate of heat transfer at the cylinder wall as time passes. The rate of heat transfer (at the wall of the cylinder) is shown to change direction regularly in the figure 12. Due to the Pr and ω effects, the rate of heat transfer on the surface of the cylinder increases in both figures.

The profiles of Sherwood number versus time t, which determines the rate of mass transfer on the cylinder's surface, are shown in Figures 14 and 15. Figure 14 shows the effect of the frequency parameter on the rate of mass transfer into the fluid. The magnitude of the rates of mass transfer on the surface of the cylinder increases as the frequency parameter is increased, as shown in diagram 14. Because the pressure gradient is a periodic function of time, the behaviour of the rate of mass transfer under the influence of Sc is periodic, as shown in Figure 15. This graph shows an increase in the rate of mass transfer due to an increase in Sc.

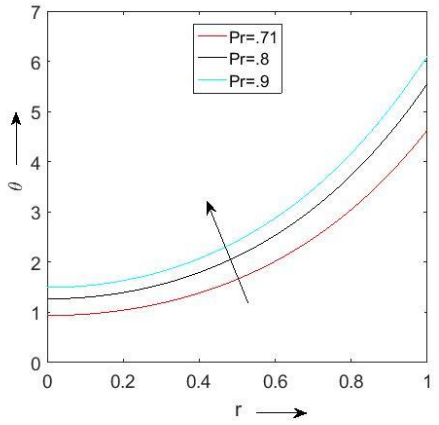

Figure 2. Temperature versus r for variation in Pr when

$N = 6, \omega = 5, Sc = .6, n_1 = 1, t = 2$

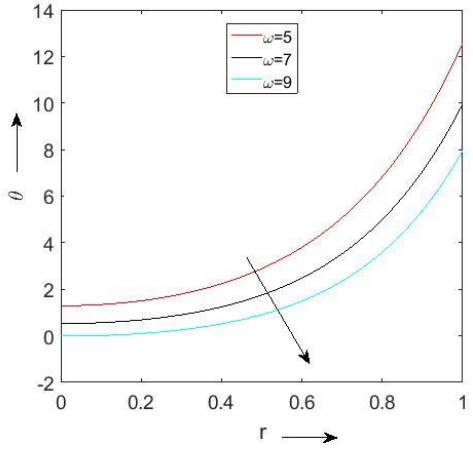

Figure 3. Temperature versus r for variation in ω when

$\Pr = .71, N = 6, Sc = 1, n_1 = 1, t = 2$

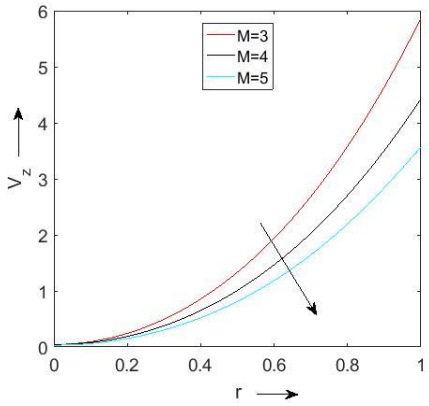

Figure 4. Velocity versus r for variation in M when

$Gr = 10, Gm = 10, \Pr = .71, N = 5,$
$\omega = 5, Sc = 1, V_o = 1, P_o = 1, n_1 = 1, t = 2$

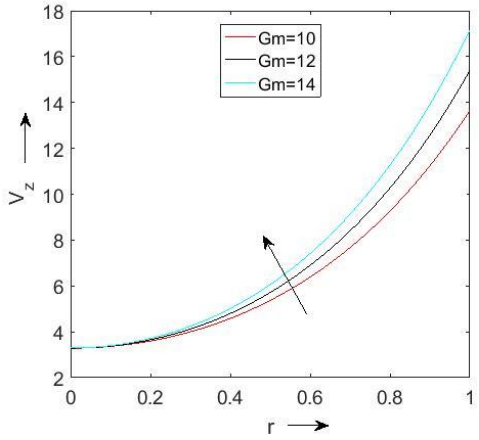

Figure 5. Velocity versus r for variation in Gm when

$Gr = 10, \Pr = .71, N = 5, M = 1,$
$\omega = 5, Sc = 1, V_o = 1, P_o = 1, n_1 = 1, t = 2$

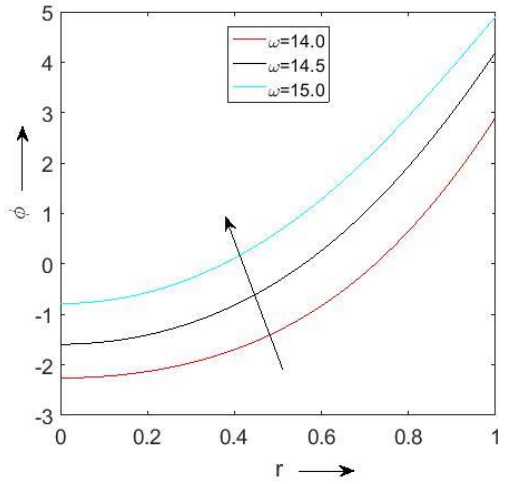

Figure 6. Concentration versus r for variation in ω when

$Sc = .6, n_1 = 5, t = .6$

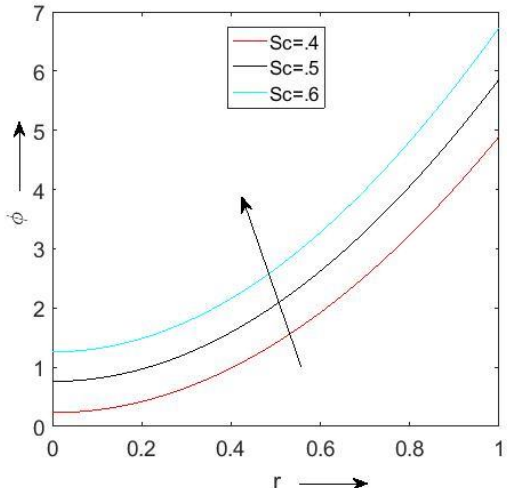

Figure 7. Concentration versus r for variation in Sc when

$\omega = 5, n_1 = 5, t = .6$

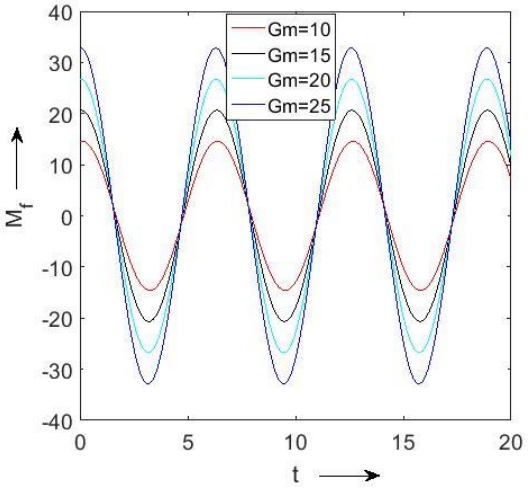

Figure 8. Mass flux versus t for variation in Gm when

$Gr = 10, \Pr = .71, N = 1, M = 1,$
$\omega = 1, Sc = .22, V_o = 1, P_o = 1, n_1 = .01, t = .2$

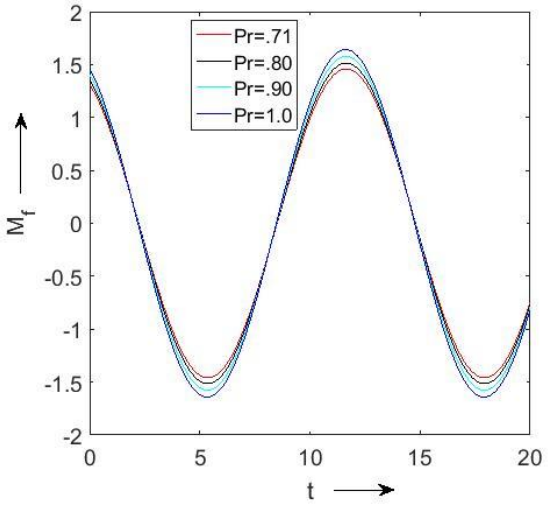

Figure 9. Mass flux versus t for variation in Pr when

$Gr = 10, Gm = 10, N = 1, M = 1,$
$\omega = 1, Sc = .22, V_o = 1, P_o = 1, n_1 = .01, t = .2$

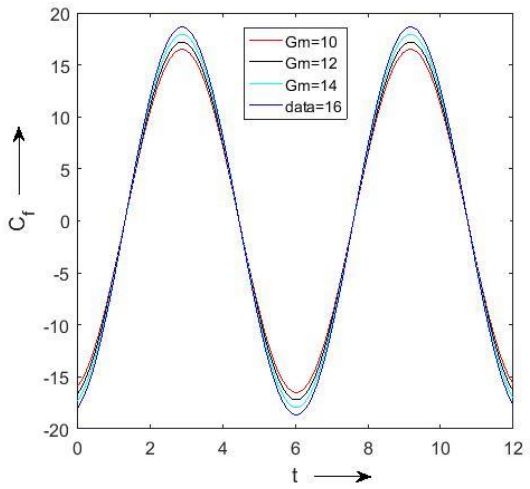

Figure 10. Skin friction versus t for variation in Gm when

$Gr = 10, \Pr = .71, N = 5, M = 1,$
$\omega = 1, Sc = .6, V_o = 1, P_o = 1, n_1 = 1, t = 2$

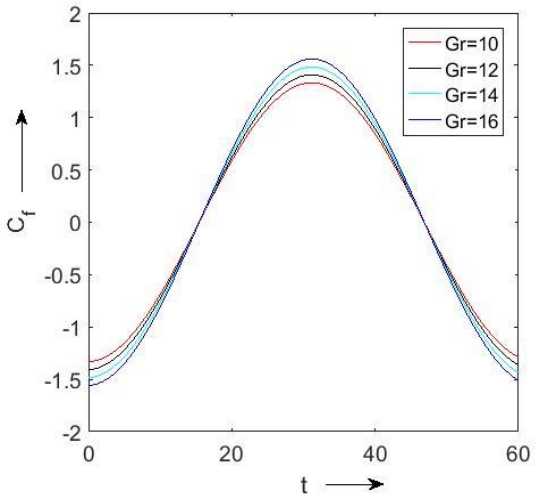

Figure 11. Skin friction versus t for variation in Gr when

$Gm = 10, \Pr = .71, N = 5, M = 1,$
$\omega = 1, Sc = .6, V_o = 1, P_o = 1, n_1 = 1, t = 2$

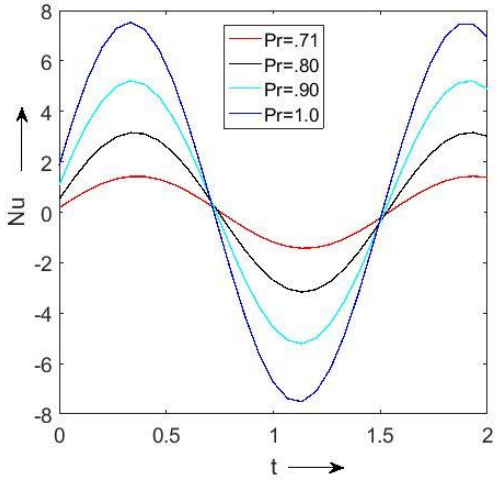

Figure 12. Nusselt number versus t for variation in Pr when

$N = 1, \omega = 4, n_1 = 1$

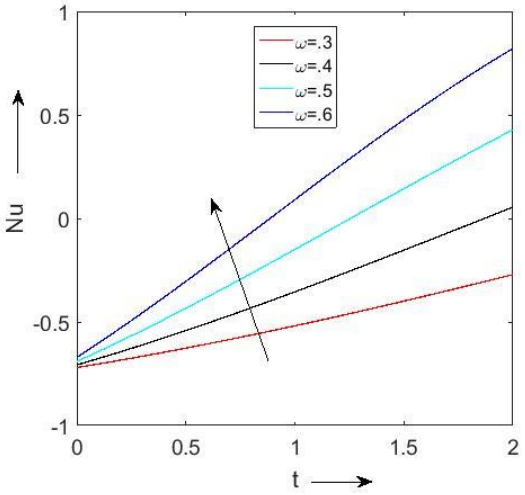

Figure 13. Nusselt number versus t for variation in ω when

$\Pr = .71, N = 1, n_1 = 1$

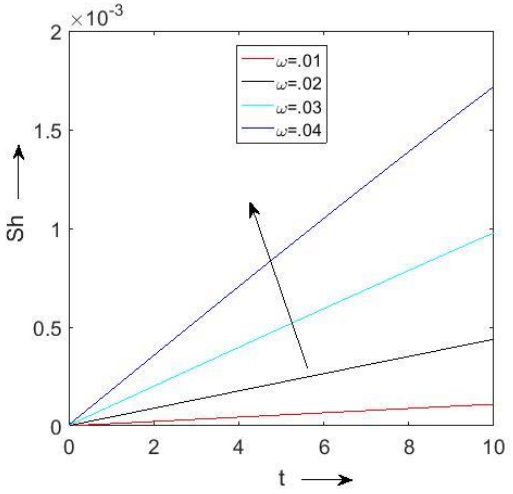

Figure 14. Sherwood number versus t for variation in ω when

$Sc = .22, n_1 = 1$

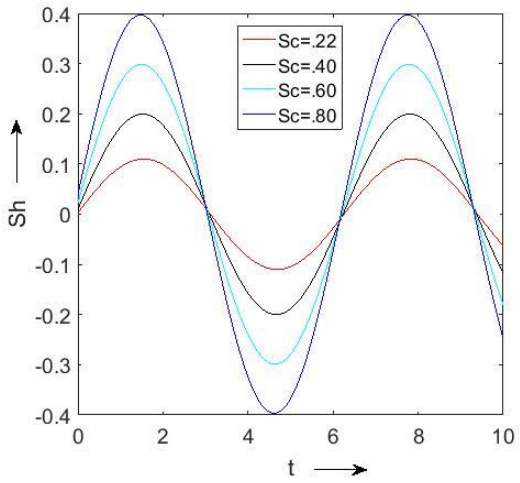

Figure 15. Sherwood number versus t for variation in Sc when

$\omega = 5, n_1 = 1$

10. CONCLUSIONS

The following are the key findings of the previous investigation:

- The fluid temperature falls under the influence of thermal diffusivity and frequency parameter.
- The fluid velocity increases as the solutal Grashof number rises, but the opposite is true as the magnetic parameter rises.
- Increase the mass diffusivity associated with the fluid flow to decrease species concentration.
- The mass flux is increased by the solutal buoyancy force, while themal diffusivity has the opposite effect.
- With increasing solutal and thermal Grashof numbers, the level of viscous drag in the fluid increases.
- The rate of heat transfer and mass transfer increases as the frequency parameter is increased.

NOMENCLATURE

a radius of the cylinder, m

$\vec{B}$ magnetic flux density

B_o strength of the applied magnetic field, Tesla

C species concentration, $Kmol / m^3$

C_S fluid concentration in static condition, $Kmol / m^3$

C_p specific heat at constant pressure, $Joule / (kg \times K)$

D_M molecular mass diffusivity, $m^2 s^{-1}$

$e_{b\lambda}$ Planck function

g acceleration due to gravity, ms^{-2}

Gr thermal Grashof number

Gm solutal Grashof number

$\vec{J}$ current density vector

κ thermal conductivity, W / mK

$\left(K_{\lambda'}\right)_w$ absorption coefficient

M magnetic parameter

M_f mass flux

n_1 amplitude

p' fluid pressure, $Newton / m^2$

p_S fluid pressure in static condition, $Newton / m^2$

p_o amplitude of the pressure gradient

Pr Prandtl number

$\vec{q}$ velocity vector

$\vec{q}_r$ radiative heat flux vector

q_r radiative heat flux, W / m^2

N radiation parameter

Sc Schmidt number

t' time, s

T temperature, K

T_S temperature of the fluid in static condition, K

Greek symbols

ω dimensionless frequency parameter

ω' dimensional frequency parameter,

β coefficient of volume expansion for heat transfer, $1/K$

$\overline{\beta}$ coefficient of volume expansion for mass transfer, $1/Kmol$

$\overline{\phi}$ viscous dissipation of energy per unit volume, $J / m^3 s$

θ non-dimensional temperature

μ coefficient of viscosity, kg / ms

μ_e magnetic permeability, $Weber / Am$

ν kinematic viscosity, $m^2 s^{-1}$

σ electrical conductivity, $(ohm \times meter)^{-1}$

ρ fluid density, kg / m^3

ρ_S fluid density in static condition, kg / m^3

CONFLICT OF INTERESTS

The author(s) declare that there is no conflict of interests.

REFERENCES

[1] R. Kumari, J.L. Bansal, Slow magnetohydrodynamic flow past a circular cylinder, Proc. Indian Acad. Sci. (Math. Sci.). 94 (1985), 51–60.

[2] D.G. Drake, On the flow in a channel due to a periodic pressure gradient, Quart. J. Mech. Appl. Math. 18 (1965), 1–10.

[3] S.V.K. Varma, K.J. Pillai, B. Ramlinca, M. Syam Babu, Unsteady flow of a viscous conducting fluid through a circular cylinder, Proc. Indian Soc. Theor. Appl. Mech. (1994), 11-20.

[4] M.Y. Antimirov, A.A. Kolyshkin, Non-stationary MHD flow in annular channel in a radial magnetic field, Magnetohydrodynamics, 20 (1984), 285-287.

[5] W.F. Hughes, F.L. Young, Electromagnetodynamics of fluids, John Wiley and Sons, New York, 1966.

[6] M. Sankar, M. Venkatachalappa, I.S. Shivakumara, Effect of magnetic field on natural convection in a vertical cylindrical annulus, Int. J. Eng. Sci. 44 (2006), 1556–1570.

[7] R.K. Jain, K.N. Mehta, Laminar hydromagnetic flow in an annulus with porous walls, Phys. Fluids, 5 (1962), 1207-1211.

[8] S. Globe, Laminar steady state magnetohydrodynamic flow in an annular channel, Phys. Fluids, 2 (1959), 404-407.

[9] A.J. Chamkha, Unsteady laminar hydromagnetic fluid particle flow and heat transfer in channels and circular pipes, Int. J. Heat Fluid Flow, 21 (2000), 740-746.

[10] K.D. Singh, Exact solution of MHD mixed convection periodic flow in a rotating vertical channel with heat radiation, Int. J. Appl. Mech. Eng. 18 (2013), 853-869.

[11] C. Israel-Cookey, E. Amos, C. Nwaigwe, MHD oscillatory couette flow of a radiating viscous fluid in a porous medium with periodic wall temperature, Amer. J. Sci. Ind. Res. 1 (2010), 326-331.

[12] T.S. Reddy, M.C. Raju, S.V.K. Varma, Unsteady MHD free convection oscillatory couette flow through a porous medium with periodic wall temperature in presence of chemical reaction and thermal radiation, Int. J. Sci. Adv. Technol. 1(10) (2011), 51-58.

[13] G.R. Machireddy, Chemically reactive species and radiation effects on MHD convective flow past a moving vertical cylinder, Ain Shams Eng. J. 4 (2013), 879-888.

[14] P. Ganesan, P. Loganathan, Radiation and mass transfer effects on flow of an incompressible viscous fluid past a moving vertical cylinder, Int. J. Heat Mass Transfer, 45 (2002), 4281-4288.

[15] R. Srinivasa Raju, M.A. Kumar, K. Sarada, Y.D. Reddy, Influence of thermal radiation on unsteady free convection flow of water near 4ºC past a moving vertical plate, Glob. J. Pure Appl. Math. 11(2) (2015), 237-240.

[16] M. Gundagani, S. Sheri, A. Paul, M.C.K. Reddy, Radiation Effects on an unsteady MHD convective flow past a semi-infinite vertical permeable moving plate embedded in a porous medium with viscous dissipation, Walailak J. Sci. Tech. 10(5) (2013), 499-515.

[17] V.S. Rao, L.A. Babu, R.S. Raju, Finite element analysis of radiation and mass transfer flow past semi-infinite moving vertical plate with viscous dissipation, J. Appl. Fluid Mech. 6(3) (2013), 321-329.

[18] N. Ahmed, M. Dutta, Heat transfer in an unsteady MHD flow through an infinite annulus with radiation, Bound. Value Probl. 2015 (2015), 11.

[19] N. Ahmed, Soret and Dufour effects in steady flow of a viscous conducting fluid through a circular cylinder, J. Energy Heat Mass Transfer, 36 (2014), 165-182.

[20] A.C. Cogley, W.G. Vincent, S.E. Gilles, Differential approximation for radiative transfer in a nongrey gas near equilibrium, AIAA J. 6 (1968), 551–553.